RSC Advances

PAPER

View Article Online
View Journal | View Issue

Cite this: *RSC Adv.*, 2018, **8**, 29356

Quinic acid and hypervalent chromium: a spectroscopic and kinetic study†

María Florencia Mangiameli, *[ab] Sebastián Bellú,[ab] Bárbara Pérez Mora,[ab] Luis Sala[a] and Nadia Mamana[a]

Received 3rd May 2018
Accepted 9th July 2018

DOI: 10.1039/c8ra03809k

rsc.li/rsc-advances

The redox reaction between an excess of quinic acid (**QA**) and Cr^{VI} involves the formation of intermediates, namely, Cr^{IV} and Cr^{V} species, which in turn react with the organic substrates. As observed with other substrates that have already been studied, Cr^{IV} does not accumulate during this reaction because of the rate of the reaction. Its rate of disappearance is several times higher than that of the reaction of Cr^{VI} or Cr^{V} with **QA**. Kinetic studies indicate that the redox reaction proceeds *via* a combined mechanism that involves the pathways $Cr^{VI} \rightarrow Cr^{IV} \rightarrow Cr^{II}$ and $Cr^{VI} \rightarrow Cr^{IV} \rightarrow Cr^{III}$, which is supported by the observation of superoxo-Cr^{III} (CrO_2^{2+}) ions, free radicals, and oxo-Cr^{V} species as intermediates and the detection of Cr^{VI} ester species. The present study reports the complete rate laws for the **QA**/chromium redox reaction.

Introduction

Cr^{VI} is a very important environmental pollutant and a well-known occupational contaminant.[1] Although it is not doubted that Cr^{VI} induces cancer,[2–8] there is still a discussion regarding the species most probably responsible for cell damage and the mechanism(s) involved.[9–12] Cr^{VI} itself cannot react with DNA *in vitro* or with isolated nuclei. On the other hand, when reducing agents are present in the medium, it causes an extensive diversity of DNA damage, which includes damage to Cr–DNA complex, DNA–protein crosslinks, and apurinic–apyrimidinic sites as well as oxidative damage.[11,13–17] The formation of Cr^{V} and $Cr^{II/IV}$ intermediates during the oxidation of a variety of organic compounds by Cr^{VI} has been observed,[18–22] and their involvement in Cr-induced cancers[1,23] has aroused much curiosity in the chemistry and biochemistry of chromium.[24] In fact, the detection by continuous-wave electron paramagnetic resonance (CW-EPR) or electron spin resonance (ESR) of a long-lived Cr^{V} species[25–28] is focused on the probable role(s) performed by Cr^{V} species in carcinogenesis brought about by Cr^{VI}. A similar situation has arisen with Cr^{IV}. In the course of the examination of the interactions of aldohexoses[29–34] and carboxylic acids[26,35–37] with Cr^{VI}, we were able to demonstrate the interactions of Cr^{VI}, Cr^{V} and Cr^{IV} with different sugars present in biological systems.

tert-2-Hydroxy acid, quinic acid (**QA**), ((1*R*,3*R*,4*R*,5*R*)-1,3,4,5-tetrahydroxycyclohexanecarboxylic acid) (Fig. 1) is a natural cyclic polyol compound found in plums, peaches, pears, apples, quina bark, *Eucalyptus globulus*, carrot and tobacco leaves, coffee beans and other vegetables.[38] Additionally, **QA** is related to the acidity of coffee.[39] **QA** is an important biological substrate, because it is important in the cellular synthesis of aromatic compounds, and it is also a multipurpose chiral starting material for new pharmaceuticals.

Considering its structure, **QA** is a perfect ligand for studying the redox reactions of Cr *in vitro* with biologically significant donor groups. The hydroxyl-substituted cyclohexane ring in **QA** can act as a cellular carbohydrate. Functional groups such as diols (*e.g.*, ascorbic acid, ribose, D-glucose and their derivatives) and 2-hydroxy acids (*e.g.*, citric, malic, and lactic acids) can be simulated by different regions of **QA** (*tert*-2-hydroxyacid moiety and *cis*-diol (O(3),O(4)) and *trans*-diol (O(4),O(5)) groups), each of which is a potential chelating agent for $Cr^{V/IV}$. It has been established that Cr^{IV}/Cr^{V} can be produced intracellularly during the reduction of Cr^{VI}[40–42] besides the oxidation of Cr^{III} in the presence of activated oxygen generated throughout enzymatic reactions.[43–46] Additionally, the lifetimes of identified Cr^{IV} complexes under biological conditions (pH ~ 7) are measured in minutes or seconds[18,47] as well as in a slightly acidic medium (pH ~ 4.5–5.5) similar to that occurring in the cellular uptake of insoluble chromates by phagocytosis.[48] **QA** makes it possible to

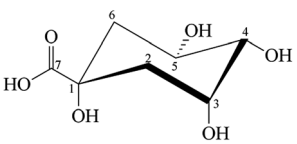

Fig. 1 The structure of **QA**.

[a]*Área Química General e Inorgánica, Departamento de Química-Física, Facultad de Ciencias Bioquímicas y Farmacéuticas, Universidad Nacional de Rosario, Suipacha 531, S2002LRK Rosario, Santa Fe, Argentina. E-mail: mangiameli@iquir-conicet.gov.ar; Tel: +54 341 4350214*

[b]*Instituto de Química de Rosario-CONICET, Suipacha 570, S2002LRK Rosario, Santa Fe, Argentina*

† Electronic supplementary information (ESI) available. See DOI: 10.1039/c8ra03809k

perform intramolecular competition experiments between different functional groups (vic-diol *versus tert*-2-hydroxy acid) or different orientations of the same functional group (*trans versus cis* diol).[49] Lay *et al.* studied **QA** by CW-EPR in the presence of Cr^{V} to determine and understand the structures of the complexes formed between both species.[49] However, no kinetic studies have been carried out on **QA**/Cr systems, which are necessary to obtain information about what is known about this substrate and its relation with chromium species and to propose a mechanism for the reaction between Cr^{VI} and **QA**. It is also important to measure the half-lives of intermediate species as well as their interaction with **QA** because of their possible presence in the intracellular environment and the potential for damage that they represent.

Experimental section

Materials

QA (Sigma, p.a.), potassium dichromate (Mallinckrodt), perchloric acid (Baker, A.C.S.), sodium hydroxide (Cicarelli, p.a.), H_2SO_4 (Fluka, puriss. p.a. (HPLC)), methanol, oxalic acid (Biopack, p.a.), HCl (Cicarelli, p.a.), argon (99.9%), acrylamide (Merck, 99.0%), ehba = 2-ethyl-2-hydroxybutanoic acid (Aldrich, 99.0%), diphenylpicrylhydrazyl (dpph) (Aldrich, p.a.), Zn (Sigma-Aldrich, 99.9%), $HgCl_2$ (Merck, 99.8%), $Cr(ClO_4)_3 \cdot 6H_2O$ (Sigma-Aldrich, p.a.) and $[Fe(NH_4)_2]_2(SO_4)_2$ (Cicarelli, p.a.) were used without further purification. Sodium perchlorate monohydrate (Fluka, 98.0%), oxygen (99.99%), Zn (Cicarelli, p.a.), and $HgCl_2$ (Cicarelli, p.a.) were also used. 4-(2-Hydroxyethyl)-1-piperazineethanesulfonic acid (Hepes) buffer (Sigma Ultra, 99.5%) was added to adjust the pH of solutions to 7.05. Aqueous solutions were prepared in Milli-Q water (18.2 MΩ cm^{-1}). $[Co^{III}(NH_3)_5Cl]Cl_2$ (ref. 50) and $Na[Cr^{V}O(ehba)_2]\cdot H_2O$[51] were synthesized according to the method described in the literature.

For experiments performed in the pH range of 1–5, the pH of the solutions was adjusted by the addition of 0.5 M $HClO_4$ or 1.0 M NaOH. In the experiments performed at a constant ionic strength (I = 1.0 M) and different proton concentrations, mixtures of sodium perchlorate solutions and perchloric acid solutions were used. Sodium perchlorate solutions were prepared by dissolving the salt in an appropriate amount of water to reach a concentration of 7.12 M. The concentration of stock solutions of perchloric acid was determined by titration employing standard analytical methods.

CAUTION. Cr^{VI} compounds are human carcinogens, and Cr^{V} complexes are mutagenic and potential carcinogens.[52] Contact with the skin and inhalation must be avoided. Acrylamide is a carcinogen and must be handled in a well-ventilated fume hood.[53]

Methods

Substrate stability

The stability of the organic substrates under different experimental conditions such as the concentrations of $HClO_4$ and oxygen used in the kinetic measurements was tested by high-performance liquid chromatography (HPLC). Chromatograms were obtained using a KNK-500A chromatograph equipped with a 7125 HPLC pump. The analysis was carried out on an Aminex HPX-87H HPLC column (300 × 7.8 mm, Bio-Rad Laboratories) using 9.0×10^{-3} N H_2SO_4 with a flow rate of 0.6 mL min^{-1} as the eluent at 33 °C. The effluent was monitored with a UV detector (ProStar 325 UV-vis detector, λ = 220 nm). **QA** was incubated at 33 °C in the conditions of the kinetic experiments. At different times, aliquots were taken, diluted with the eluent medium and filtered using a nylon filter with 0.2 μm pores (Nalgene) prior to injection.

Polymerization test

The polymerization of acrylamide was investigated during the reaction of **QA** with Cr^{VI} by employing a specific test for the generation of free radicals.[54] A solution of Cr^{VI} (0.19 mL, 0.53 M) was added to 1.0 mL of a reaction mixture containing **QA** (1.0 mmol) and acrylamide (3.66 mmol). When $[Cr^{VI}]$ was negligible, 5.0 mL of cold methanol (0 °C) was added to the mixture, and a white polymer precipitated. Control experiments showed that no polymerization of acrylamide occurred under the experimental conditions with either Cr^{VI} or **QA** alone. The reaction of oxalic acid with Cr^{VI} was employed as a positive control. A solution of Cr^{VI} (1.0 mL, 0.53 M) was added to 1.0 mL of a mixture containing oxalic acid (2.0 mmol) and acrylamide (7.3 mmol). After the disappearance of Cr^{VI}, 10.0 mL of cold methanol (0 °C) was added to the reaction mixture, and the immediate appearance of a white polymer was observed. Possible reactions of Cr^{V} and Cr^{IV} with acrylamide were investigated using $Na[Cr^{V}O(ehba)_2]$[54] and $[Cr^{IV}O(ehbaH)_2]$.[50] No precipitation occurred upon mixing Cr^{V} or Cr^{IV} complexes with acrylamide under the conditions used in the Cr^{VI}/**QA** reaction.

Generation of Cr^{II}

As was previously described in the main text,[18,26,27,37] aqueous CrO^{2+} species can be generated *in situ* by rapid oxidation of Cr^{2+} using oxygen. To generate the required Cr^{2+}, it is necessary to employ a highly reducing medium. The procedure involves a Zn/Hg amalgam and a strong flow of hydrogen. The Zn/Hg amalgam was prepared in a 5 mL balloon by stirring a mixture of Zn (~5.0 g, previously washed with 3.0 M HCl for 5 min) and $HgCl_2$ (0.3 M in 1.0 M HCl) for 30 min. Afterwards, excess $HgCl_2$ was eliminated, and the resulting amalgam was washed three times with 1.0 M $HClO_4$ and finally with distilled water. An appropriate volume of $HClO_4$ and distilled water was added to the amalgam in the balloon to obtain pH of 1.0 in a final volume of 3.5 mL. Finally, the balloon was closed with a rubber septum cap and stirred while being bubbled with H_2 for at least 45 min to ensure a reducing medium. Then, 200 μL of 6.0 mM $Cr(ClO_4)_3$ was injected while keeping the H_2 bubbling and stirring constant. After 1.0 h, $Cr(ClO_4)_3$ was quantitatively reduced to Cr^{2+}. The value of $[Cr^{2+}]$ was determined by treating an aliquot of the reaction mixture with an aqueous solution of $[Co^{III}(NH_3)_5Cl]Cl_2$ under an anaerobic atmosphere (Ar); the mixture was then poured into concentrated HCl, and the Co^{II} content was determined by measuring the absorbance of $[CoCl_4]^{2-}$ at 692 nm.[50]

In situ generation of oxo-Cr^{IV} (CrO^{2+})

For *in situ* generation of CrO^{2+}, a deoxygenated solution of Cr^{2+} was injected into an acidic aqueous solution of **QA**, which was saturated with O_2 (1.26 mM). At very low Cr^{2+}/O_2 ratios (<0.05), CrO_2^{2+} was quantitatively formed, whereas at intermediate Cr^{2+}/O_2 ratios (~0.15), the reaction afforded mixtures of CrO^{2+} and CrO_2^{2+}.[55] In a typical experiment, 100 μL of 6.0 mM Cr^{2+} was injected into a septum-capped spectrophotometric quartz cell with a path length of 1.0 cm, which was filled with 2.3 mL of an O_2-saturated solution containing 0.25–6.0 mM **QA** and appropriate concentrations of $HClO_4$ and $NaClO_4$ ($[H^+] = 0.1$–0.6 M, $I = 1.0$ M) at 15 °C. Under these experimental conditions, the reaction between Cr^{2+} and O_2 rapidly produced 0.07 mM CrO^{2+} (average yield of 28% based on total $[Cr^{2+}]$). After CrO^{2+} was formed, it reacted with **QA** to yield Cr^{2+}, which was then quantitatively transformed to a superoxo-Cr^{III} ion (CrO_2^{2+}) by reacting with the remaining oxygen (Cr^{2+}/O_2 ratio <0.05) with no autocatalytic consumption of CrO_2^{2+} by Cr^{2+}.[55]

Quantification of CrO^{2+}

The concentration of CrO^{2+} generated by the reaction of Cr^{2+} with O_2 was determined by injecting 100 μL of 6.0 mM Cr^{2+} into 2.3 mL of an O_2-saturated solution of 0.1 M ehba buffer (pH 3.0) at 15 °C. Immediately after mixing, the solution turned pink, and the absorbance of $[Cr^{IV}(O)(ehba)_2]^{2-}$ at 512 nm (ε = 2380 M^{-1} cm^{-1}) was measured.[47]

Spectrophotometric measurements

All kinetic measurements were performed by monitoring the absorbance changes with a Jasco V-550 spectrophotometer with fully thermostated cell compartments (±0.2 °C). The reactions were followed under pseudo-first-order conditions using an excess of **QA** with respect to Cr. The reactant solutions were thermostated prior to the experiment and transferred into a quartz cell with a path length of 1.0 cm immediately after mixing. All kinetic data were fitted using routines in the Origin 6.0 package.

Table 1 lists key wavelengths for different Cr species analyzed in this study.

Chromate esters

Chromate esters were investigated by UV-vis spectrophotometry in the region of 250–600 nm, in which they exhibited characteristic absorption bands. Reactions were performed at pH of 7.05 (Hepes buffer), at which the redox reaction is slow enough to enable observations of the formation of esters. The instrument was zeroed using an arrangement in which the reference and sample beams passed through matching cells, and both contained 5.0×10^{-4} M Cr^{VI} in 0.1 M Hepes buffer with a pH of 7.05. The solution in the sample cell was replaced with a reaction solution containing 5.0×10^{-4} M Cr^{VI} and 0.25–0.013 M **QA** in Hepes buffer at pH = 7.05 and $T = 24$ °C. The spectra obtained after mixing showed a characteristic absorption at 460 nm. Each mixture was monitored for 5 minutes, and no variations were observed in the shape and intensity of the spectra.

Table 1 Wavelengths for different Cr species

Chromium species	Cr^{VI}	Cr^{V}	Cr^{III}	CrO_2^{2+}
Wavelength (nm)	350	570	570	290

Time evolution of the QA/Cr^{VI} reaction

Time-dependent UV-vis spectra were recorded for two different reaction mixtures. The first mixture containing 0.3 M **QA**, 0.1 M $HClO_4$, and 6.0×10^{-4} M Cr^{VI} with $I = 1.0$ M at 33 °C was monitored between 200 and 800 nm every 4 minutes until total consumption of Cr^{VI} to determine the presence of the isosbestic point. The second reaction mixture containing 0.3 M **QA**, 0.1 M $HClO_4$, and 6.0×10^{-3} M Cr^{VI} with $I = 1.0$ M at 33 °C was monitored between 450 and 900 nm every 4 minutes until total consumption of Cr^{VI} to determine whether the final redox product of the reaction was $Cr^{III}_{(aq)}$ or Cr^{III} ligand. In this reaction, the time evolution of the **QA**/Cr^{VI} mixture was monitored by following changes in the absorption band at 570 nm. The concentration of Cr^{VI} used in this experiment was 10 times higher because Cr^{III} species have a very low ε value at 570 nm. The rate constants obtained at this wavelength were in agreement with those calculated from the data recorded at 350 nm in these experimental conditions.

QA/Cr^{VI} reactions

The disappearance of Cr^{VI} in the reaction mixtures at 33 °C was followed by monitoring the absorbance at 350 nm until at least 80% conversion. The initial concentration of Cr^{VI} was 6.0×10^{-4} M, whereas the **QA** concentration was varied from 0.03 M to 0.12 M. In these kinetic measurements, I was kept constant at 1.0 M, whereas $[HClO_4]$ was varied from 0.1 to 0.5 M at various [**QA**] values. The rate constants (k_6 and k_5) were deduced from multiple determinations and were within ±10% of each other. The rate constants obtained at 350 nm were used to fit the absorbance changes at 420–440 nm. The goodness of fit at these wavelengths was used to corroborate the rate expressions used to determine the rate constants for 350 nm. The first-order dependence of the rate upon $[Cr^{VI}]$ was confirmed by a set of experiments, where $[Cr^{VI}]_0$ was varied between 0.3 and 0.6 mM, but T, [**QA**] and ionic strength were kept constant.

Detection of superoxo-Cr^{III} ions during the reaction of QA with Cr^{VI}

The fact that Cr^{II} is involved in the oxidation mechanism of several alcohols by Cr^{IV} and Cr^{VI} in $HClO_4$ was demonstrated by its conversion to CrO_2^{2+} upon reacting with dioxygen.[55–59] The possible formation of Cr^{2+} in **QA**/Cr^{VI} mixtures was investigated by periodic UV-vis scanning (220–500 nm) of solutions of 0.09 M **QA**, 0.06 mM Cr^{VI} and 1.0 M $HClO_4$ saturated with oxygen ($[O_2]$ = 1.26 mM) at 25 °C. Periodic scanning of the reaction mixture showed that the Cr^{VI} band at 350 nm decreased in intensity, whereas new peaks appeared at 290 nm and 245 nm. When the

value of [Cr^{VI}] was negligible, 0.30 mM Fe^{2+} was added to bring about the following reaction (eqn (1)):

$$CrO_2^{2+} + 3Fe^{2+} + 4H^+ \rightarrow Cr^{3+} + 3Fe^{3+} + 2H_2O \quad (1)$$

The spectrum of the reaction mixture was subtracted from the corresponding spectrum recorded prior to the addition of Fe^{2+}. The presence of a negative difference in absorbance around 290 nm between these spectra was consistent with the presence of CrO_2^{2+}.

In addition, the same reaction was conducted under strictly anaerobic conditions (Ar). In this case, the absence of oxygen implied that no Cr^{IV} would be generated and also no CrO_2^{2+} would be formed. The characteristic absorption bands at 245 and 290 nm were not present.

QA/Cr^{IV} reactions

The oxidation of **QA** by CrO^{2+} was studied under pseudo-first-order conditions with an excess of **QA** with respect to Cr^{IV} and monitored using a spectrophotometer by following CrO_2^{2+} as a final redox product. Kinetic data were recorded spectrophotometrically following the formation of CrO_2^{2+} at 290 nm (ε = 3000 M^{-1} cm^{-1}) by employing a septum-capped spectrophotometer cell with a path length of 1.0 cm, which was filled with 2.3 mL of an O_2-saturated solution of the organic substrate. At this wavelength, neither the substrate **QA** nor the oxidized products exhibited absorption. All mixtures of **QA**/CrO^{2+} showed an increase in two absorption bands (245 and 290 nm) with a relative intensity of Abs_{245}/Abs_{290} = 2.2, which is characteristic of CrO_2^{2+}.[55] Kinetic measurements were performed at [Cr^{IV}] = 0.07 mM, I = 1.0 M, [O_2] = 1.26 mM and 15 °C. The range of **QA** concentrations used was 1.0–6.0 mM, and no disproportionation reaction of CrO^{2+} was observed. The range of [$HClO_4$] used was 0.10–0.60 M. The experimental pseudo-first-order rate constants (k_{4exp}), which were determined from nonlinear least-square fits of absorbance data for 290 nm, were the averages of at least five determinations and were within ±10% of each other. The data used to calculate the kinetic constant, k_{4exp}, corresponded to 80% of the exponential growth in the experimental values. The first-order dependence of the rate upon [Cr^{IV}] was confirmed by a set of experiments, where [Cr^{IV}]$_0$ was varied between 3.0×10^{-5} and 6.0×10^{-5} M, but T, [**QA**], and I were kept constant.

EPR measurements

EPR spectra were obtained with a Bruker Elexsys 500 spectrometer operated at X-band frequencies (~9 GHz). Microwaves were generated by means of a klystron (ER041MR), and frequencies were measured with a built-in frequency counter. Spectra were recorded as first derivatives of the microwave absorption at 1024 points at 18 ± 1 °C using a microwave power of 202 mW, a modulation amplitude of 2.0 G, a time constant of 20 ms, a sweep width of 120 G and a conversion time of 40 ms. Also, g-values were determined by reference to dpph (g = 2.0036) as an external standard reference. The power values used in the EPR experiments did not exceed 10 mW to avoid signal saturation. In the EPR measurements, the speed and number of scans were fixed to reduce the time taken for each measurement; this was done to avoid fluctuations in the EPR signals during scanning of the samples.

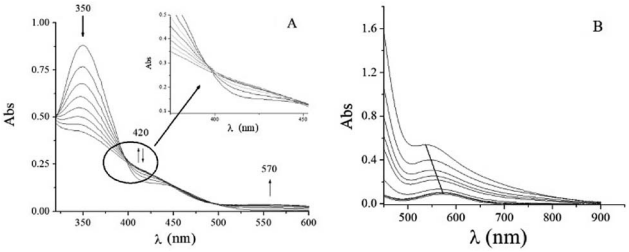

Fig. 2 Time evolution of the **QA**/Cr^{VI} reaction as followed by UV-vis absorption spectroscopy. Time evolution of the **QA**/Cr^{VI} reaction at [H^+] = 0.10 M, I = 1.0 M, [**QA**] = 0.30 M, T = 33.0 °C and (A) [Cr^{VI}]$_0$ = 6.0 × 10^{-3} M or (B) [Cr^{VI}]$_0$ = 6.0 × 10^{-4} M. The first trace was recorded at t = 0 min, and the time interval between each trace was 4.0 min. (B) Shows spectra: 1–5, 10, 50, 100, 200, and 300. After 400 min (100 spectra), no changes were observed.

Results

Reaction time of the QA/Cr^{VI} mixture

The UV-vis absorption spectrum of the **QA**/Cr^{VI} reaction mixture in an acidic medium ($HClO_4$) showed the characteristic behavior of Cr^{VI} in an acidic medium[25–27] with a shoulder at 420/450 nm and a band at 350 nm (Fig. 2). The absorbance at 350 nm decayed, and the absorbance at the shoulder first increased and then decayed over time; also, there was an increase in the absorbance at 570 nm (Fig. 2A).

The absence of an isosbestic point (highlighted area in Fig. 2A) indicates that there are more than one competing redox reactions involving intermediate chromium species, which must be present in appreciable concentrations during the reduction of Cr^{VI} to Cr^{III}.

As the reaction proceeded, two d–d bands were detected in the electronic absorption spectrum at λ_{max} = 406 nm (ε = 40 M^{-1} cm^{-1}) and 573 nm (ε = 18 M^{-1} cm^{-1}) (Fig. S1†). These bands were assigned to the $^4A_{2g} \rightarrow {}^4T_{1g}$ and $^4A_{2g} \rightarrow {}^4T_{2g}$ octahedral transitions of Cr^{III} in O_h symmetry.[60] After 6 h, significant changes were observed in these two bands; for example, the band at 539 nm (ε = 90 M^{-1} cm^{-1}) shifted to 571 nm (ε = 15 M^{-1} cm^{-1}) (Fig. 2B). This observation suggested that the absorption at 571 nm originated from Cr^V and Cr^{III}–**QA** complex species. The Cr^{III}–**QA** complex formed initially was slowly hydrolysed to $Cr^{III}_{(aq)}$.

Detection of Cr^{VI} esters

Differential UV-vis spectra of **QA**/Cr^{VI} mixtures were used to study the formation of Cr^{VI} esters. An absorption band (λ_{max} = 470 nm) was observed (Fig. 3), which was consistent with literature data.[61] At pH values near neutrality, the redox reaction of **QA**/Cr^{VI} occurred extremely slowly, and the reduction of Cr^{VI} was negligible. In consequence, the ester formation and electron transfer reactions could be clearly distinguished.

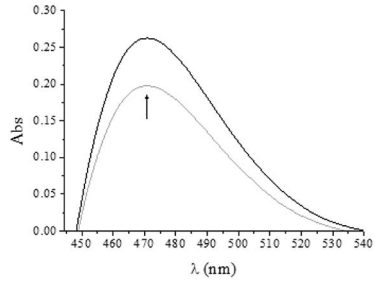

Fig. 3 Differential UV-vis spectra of QA/Cr^{VI} mixtures at pH of 7.05: [QA] = 0.25 M (black)–0.013 M (grey), [Cr^{VI}] = 5.0×10^{-4} M, [Hepes] = 0.10 M, T = 24.0 °C, and pH = 7.05.

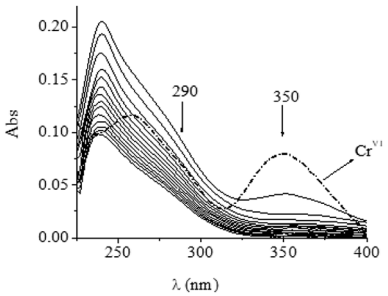

Fig. 5 Time evolution of the anaerobic QA/Cr^{VI} mixture. [H^+] = 0.10 M, I = 1.0 M, [Cr^{VI}]$_0$ = 0.07 mM, [QA] = 0.015 M, and T = 25.0 °C in the absence of oxygen. The first trace was recorded at t = 0 min, and the time interval between each trace was 2.0 min.

Detection of Cr^{II}

The involvement of Cr^{II} species in the oxidation of different organic alcohols by Cr^{IV}/Cr^{VI} in acidic media has previously been established by the formation of superoxo-Cr^{III} (CrO_2^{2+}) by a reaction with dioxygen.[18,26,27,37,55,62] Periodic scanning of the QA/Cr^{VI} reaction mixture in 1.0 M $HClO_4$ with a high oxygen concentration and a very low Cr^{VI} concentration (please see experimental conditions) reveals two bands at 290 and 245 nm, which are characteristic of CrO_2^{2+} (Fig. 4). This observation confirms the formation of Cr^{II} and can be considered to be indirect evidence of the participation of Cr^{IV} in the QA/Cr^{VI} redox mechanism, as has been observed with other saccharides.[18,25–27,37]

Taking into account the spectra shown in Fig. 4, the absorbance at 245 nm and 290 nm at any time in these experimental conditions is due to the contributions of CrO_2^{2+} and Cr^{VI}. It is interesting to determine how much each species contributes to the total absorbance to determine the real contribution of the redox reaction of Cr^{IV} to the total oxidation mechanism. To do this, the contribution of CrO_2^{2+} ions at the absorbance at 245 nm is calculated according to eqn (2):

$$Abs_{245}(CrO_2^{2+}) = Abs_{245} - Abs_{350} \times \varepsilon_1^{-1} \times \varepsilon_2 \quad (2)$$

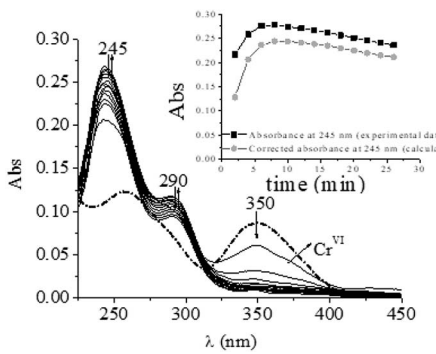

Fig. 4 Time evolution of the QA/Cr^{VI} mixture saturated with dioxygen. [H^+] = 0.10 M, I = 1.0 M, [Cr^{VI}]$_0$ = 0.07 mM, [QA] = 0.015 M, T = 25.0 °C, and [O_2] = 1.26 mM. The first trace was recorded at t = 0 min, and the time interval between each trace was 2.0 min. Inset: evolution of [CrO_2^{2+}] with time in black (experimental data) and grey (calculated data).

here, ε_1 and ε_2 are the molar absorption coefficients of Cr^{VI} at 350 nm and 245 nm, respectively. Under our experimental conditions, the molar absorptivity values were ε_1 = 1550 M^{-1} cm^{-1} and ε_2 = 1900 M^{-1} cm^{-1}. The inset in Fig. 4 indicates time evolution of [CrO_2^{2+}].

Considering that the molar absorption coefficient of CrO_2^{2+} at 245 nm is 7000 M^{-1} cm^{-1},[56] the maximum concentration of CrO_2^{2+} was 3.48×10^{-5} M (yield, 49.7%). The yield of CrO_2^{2+} should approximate to 100% if the reaction takes place entirely *via* the $Cr^{VI} \rightarrow Cr^{IV} \rightarrow Cr^{II}$ pathway. The fact that the percentage yield of CrO_2^{2+} reached only 50% of the expected theoretical value suggested that only half of Cr^{VI} reacted with **QA** *via* a pathway involving $Cr^{II/IV}$.

At 350 nm, the absorbance was insignificant; 0.30 mM Fe^{II} was added, and a new spectrum was recorded. The latter spectrum was subtracted from the spectrum recorded prior to the addition of Fe^{II}. The difference spectrum displayed a negative absorbance around 290 nm, which is consistent with the formation of CrO_2^{2+}, as has been observed with other saccharides (Fig. S2†).[18]

When the QA/Cr^{VI} reaction was conducted in the same experimental conditions but in a strictly anaerobic medium (Ar), the spectrum showed the disappearance of the characteristic bands of CrO_2^{2+} at 245 and 290 nm due to anaerobic conditions (Fig. 5). This fact also confirmed the identity of Cr^{II} species.

Rate studies

Reaction of QA/Cr^{IV}

As was reported in the experimental section, Cr^{IV} was generated *in situ* through the reaction between Cr^{II} and O_2 in appropriate experimental conditions. The QA/Cr^{IV} reaction under acidic media and O_2-saturated conditions produced Cr^{II}. Since neither the substrate nor the oxidized products absorb at 290 nm, this reaction can be indirectly observed by measuring the increment in absorbance at this wavelength, which corresponds to the formation of CrO_2^{2+}. Typical sequential electronic spectra, which show the characteristic bands of CrO_2^{2+} at 245 and 290 nm, are shown in Fig. 6A. The intensity ratio between the absorption bands at 245 and 290 nm was 2.2, which confirmed

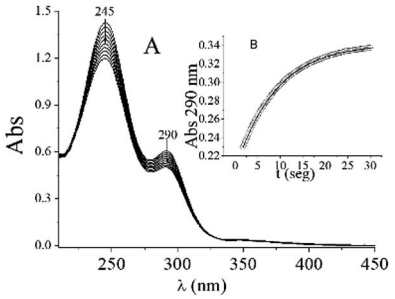

Fig. 6 (A) Time evolution of UV/vis absorption spectra of **QA**/Cr^{IV} mixtures. (B) Increase in absorbance at 290 nm due to CrO_2^{2+} formation by the **QA**/Cr^{VI} reaction. $[H^+] = 0.30$ M, $I = 1.0$ M, $[Cr^{IV}]_0 = 0.07$ mM, [**QA**] = 0.003 M, $T = 15.0$ °C, and $[O_2] = 1.26$ mM. The time interval between each trace was 2.0 min. The fitting of the experimental data was performed using eqn (2) and the Origin 6.0 program.

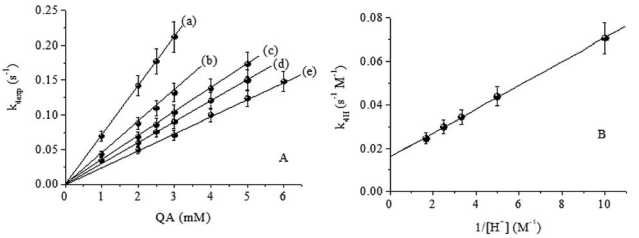

Fig. 7 (A) Effect of [**QA**] on k_{4exp}. (B) Linear dependence of k_{4H} on $[H^+]^{-1}$. $T = 15.0$ °C, $I = 1.0$ M, $[Cr^{IV}]_0 = 0.070$ mM and $[H^+]$ = (a) 0.10, (b) 0.20, (c) 0.30, (d) 0.40 and (e) 0.60 M.

the presence of CrO_2^{2+}.[18,55,56,63] As occurred with other substrates studied previously,[18,25–27,37] the monotonic growth at 290 nm was found to follow first-order kinetics (Fig. 6B). A series of experiments using constant values of temperature, [**QA**] and ionic strength (I) and $[Cr^{IV}]_0$ in the range of 3.0–6.0 × 10^{-5} M were used to confirm the first-order dependence of the rate upon $[Cr^{IV}]$ (data not shown). The experimental rate constant, k_{4exp}, was calculated by applying a nonlinear least-square fit to the absorbance/time data using 80% of the exponential growth in the experimental values, according to eqn (3):

$$Abs = Abs_\infty + (Abs_0 - Abs_\infty)e^{-(k_{4exp})t} \quad (3)$$

here, Abs_0 and Abs_∞ correspond to the initial absorbance and the absorbance at infinite time. It is known that Cr^{IV} can disproportionate into Cr^{III} and Cr^{VI} with an inverse dependence on $[H^+]$ and through second-order kinetics on $[Cr^{VI}]$.[64] This must be prevented because Cr^{VI} absorbs at 290 nm, as was previously established, which interferes with the determination of CrO_2^{2+}. At a very low concentration and in the absence of **QA**, we observed a typical spectrum of Cr^{VI} with the distinctive band at 350 nm (data not shown). For this reason, the experimental conditions were selected to avoid the disproportionation reaction of Cr^{IV}. Fitting of the time-dependent absorbance data for 290 nm using eqn (3) is shown in Fig. 6B.

Table 2 summarizes the values of k_{4exp} for several concentrations of **QA** in different concentrations of $HClO_4$. As represented in Fig. 7A, the k_{4exp} values for different $[H^+]$ values depend linearly on the concentration of **QA**. The k_{4H} values were calculated using eqn (4):

$$k_{4exp} = k_{4H}[\mathbf{QA}] \quad (4)$$

The bimolecular rate constant, k_{4H}, varies linearly with $[H^+]^{-1}$ with a slope k_{IV}^{II} of (0.00548 ± 6.4) × 10^{-5} s^{-1} and a positive intercept k_{IV}^{I} of (0.01615 ± 3.5) × 10^{-4} M^{-1} s^{-1} (Fig. 7B), according to eqn (5):

$$k_{4H} = k_{IV}^{I} + k_{IV}^{II}[H^+]^{-1} \quad (5)$$

Combining eqn (4) and (5) results in eqn (6), which describes the rate constant, k_4, for the disappearance of Cr^{IV}:

$$k_4 = (k_{IV}^{I} + k_{IV}^{II}[H^+]^{-1})[\mathbf{QA}] \quad (6)$$

Oxidation of QA by Cr^{VI}

As was previously observed with other substrates,[25–27] for the **QA**/Cr^{VI} mixture, the curves of absorbance at 350 nm *vs.* time displayed a monotonic decreasing behavior that cannot be described using a single-exponential decay. An acceptable

Table 2 Observed pseudo-first-order rate constants (k_{4exp}) for different values of $[HClO_4]$ and [**QA**][a]

	$[HClO_4]$/M				
[**QA**]/mM	0.10	0.20	0.30	0.40	0.60
1.00	0.070 ± 0.007	0.044 ± 0.004	0.035 ± 0.004	—	—
2.00	0.142 ± 0.014	0.088 ± 0.009	0.066 ± 0.007	0.060 ± 0.006	0.05 ± 0.005
2.50	0.177 ± 0.018	0.110 ± 0.011	0.086 ± 0.009	0.076 ± 0.008	—
3.00	0.212 ± 0.021	0.132 ± 0.013	0.104 ± 0.010	0.090 ± 0.009	0.074 ± 0.007
4.00	—	—	0.138 ± 0.014	0.120 ± 0.012	0.100 ± 0.010
5.00	—	—	0.173 ± 0.017	0.150 ± 0.015	0.124 ± 0.012
6.00	—	—	—	—	0.148 ± 0.015

[a] $T = 15.0$ °C, $[Cr^{IV}]_0 = 0.070$ mM, and $I = 1.0$ M. Mean values from multiple determinations. The rate constants were obtained using the Origin 6.0 program.

description of the kinetic profiles could be obtained by using a set of consecutive first-order reactions, as presented in Scheme 1.

Considering the superposition of the absorbance of Cr^{V} throughout the redox reaction, the absorbance at 350 nm is given by eqn (7):

$$Abs_{350} = \varepsilon^{VI}[Cr^{VI}] + \varepsilon^{V}[Cr^{V}] \quad (7)$$

Combining eqn (6) with rate expressions[65] that result from considering first-order reactions gives the following expression (eqn (8)):

$$Abs_{350} = Abs_0 e^{-2(k_6)t} + k_6\varepsilon^{V}[Cr^{VI}]_0(e^{-(k_5)t} - e^{-2(k_6)t})/(2k_6 - k_5) \quad (8)$$

here, ε^{V} is the molar absorptivity of oxo-Cr^{V}–**QA** at 350 nm ($\varepsilon^{V} = (1.7 \pm 0.50) \times 10^3\ M^{-1}\ cm^{-1}$), and the parameters k_5 and k_6 are the rates of disappearance of Cr^{V} and Cr^{VI}, respectively. A nonlinear iterative computer fit using eqn (8) was used to estimate both parameters k_6 and k_5. Table 3 shows the calculated values of k_6 and k_5 for different concentrations of **QA** and $HClO_4$. It is important to note that in eqn (8), k_6 appears twice in the denominator and in the exponential terms and only once in the numerator of the pre-exponential term, which is consistent with the reaction in Scheme 1, in which half of Cr^{VI} is converted to Cr^{III} *via* Cr^{V} intermediates. In the range of proton concentrations employed in this study, plots of k_6 *vs.* [**QA**] gave good straight lines (Fig. 8A). Values of k_{6H} were determined using these experimental data by eqn (9). The bimolecular rate constant, k_{6H}, exhibited variation with $[H^+]$, which can be described as quadratic dependence, as shown in Fig. 8B. This behavior can be described using eqn (10). Consequently, by combining eqn (9) and (10), k_6 can be calculated as indicated by eqn (11).

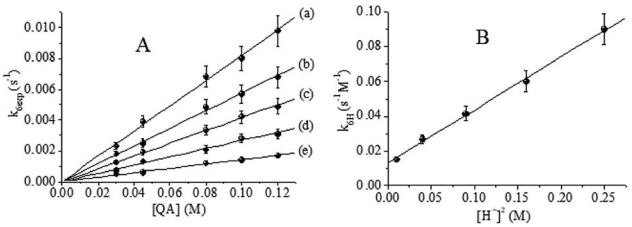

Fig. 8 (A) Effect of [**QA**] on k_{6exp}. (B) Quadratic dependence of k_{6H} on $[H^+]^2$. $T = 33.0$ °C, $I = 1.0$ M, $[Cr^{VI}]_0 = 6.0 \times 10^{-4}$ M and $[H^+]$ = (a) 0.10, (b) 0.20, (c) 0.30, (d) 0.40 and (e) 0.50 M.

$$k_{6exp} = k_{6H}[\mathbf{QA}] \quad (9)$$

$$k_{6H} = k_{VI}^{I} + k_{VI}^{II}[H^+]^2 \quad (10)$$

$$k_6 = (k_{VI}^{I} + k_{VI}^{II}[H^+]^2)[\mathbf{QA}] \quad (11)$$

here, $k_{VI}^{I} = (1.31 \pm 0.01) \times 10^{-2}\ s^{-1}\ M^{-3}$ and $k_{VI}^{II} = (3.05 \pm 0.09) \times 10^{-1}\ s^{-1}\ M^{-3}$ (Fig. 8B).

Plots of k_{5exp} *vs.* [**QA**] for a constant value of $[H^+]$ revealed linear dependence, as can be seen in Fig. 9A. Using these experimental data and eqn (12), the bimolecular rate constant k_{5H} could be calculated. A quadratic dependence was revealed by plotting k_{5H} *vs.* $[H^+]$ (Fig. 9B). The corresponding k_{5H} values were calculated using eqn (13).

$$k_{5exp} = k_{5H}[\mathbf{QA}] \quad (12)$$

$$k_{5H} = k_{V}^{I} + k_{V}^{II}[H^+]^2 \quad (13)$$

$$k_5 = (k_{V}^{I} + k_{V}^{II}[H^+]^2)[\mathbf{QA}] \quad (14)$$

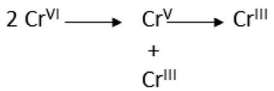

Scheme 1 $Cr^{VI} \rightarrow Cr^{III}$ reduction pathway used to fit the experimental data.

Table 3 Observed pseudo-first-order rate constants (k_{6exp} and k_{5exp}) for different values of $[HClO_4]$ and [**QA**][a]

	$[HClO_4]$/M				
[**QA**]/M	0.10	0.20	0.30	0.40	0.50
$10^3\ k_{6exp}$[b]/$s^{-1}\ M^{-1}$					
0.030	0.48 ± 0.05	0.73 ± 0.07	1.27 ± 0.13	1.80 ± 0.18	2.30 ± 0.23
0.045	0.60 ± 0.06	1.30 ± 0.13	1.90 ± 0.19	2.50 ± 0.25	3.90 ± 0.39
0.080	1.19 ± 0.12	2.10 ± 0.21	3.36 ± 0.34	4.86 ± 0.49	6.85 ± 0.69
0.100	1.40 ± 0.14	2.80 ± 0.28	4.22 ± 0.42	5.70 ± 0.57	8.00 ± 0.80
0.120	1.70 ± 0.17	3.10 ± 0.31	4.90 ± 0.49	6.80 ± 0.68	9.80 ± 0.98
$10^3\ k_{5exp}$[b]/s^{-1}					
0.030	0.11 ± 0.01	0.17 ± 0.02	0.25 ± 0.03	0.40 ± 0.04	0.70 ± 0.07
0.045	0.14 ± 0.014	0.22 ± 0.02	0.36 ± 0.40	0.60 ± 0.06	0.98 ± 0.09
0.080	0.27 ± 0.023	0.39 ± 0.04	0.62 ± 0.06	1.04 ± 0.11	1.79 ± 0.18
0.100	0.33 ± 0.03	0.48 ± 0.05	0.81 ± 0.08	1.33 ± 0.13	2.20 ± 0.20
0.120	0.40 ± 0.04	0.63 ± 0.06	0.98 ± 0.09	1.60 ± 0.16	2.70 ± 0.30

[a] $T = 33.0$ °C, $[Cr^{VI}]_0 = 6.0 \times 10^{-4}$ M, and $I = 1.0$ M. [b] Mean values from multiple determinations.

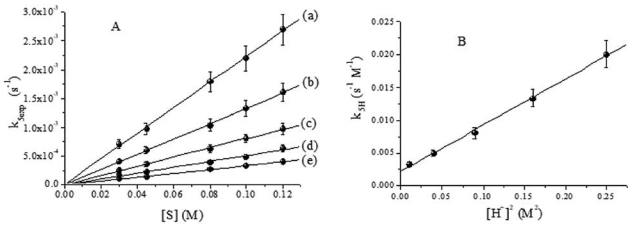

Fig. 9 (A) Effect of [QA] on k_{5exp}. (B) Quadratic dependence of k_{5H} on $[H^+]^2$. $T = 33.0$ °C, $I = 1.0$ M, $[Cr^{VI}]_0 = 6.0 \times 10^{-4}$ M and $[H^+]$ = (a) 0.10, (b) 0.20, (c) 0.30, (d) 0.40 and (e) 0.50 M.

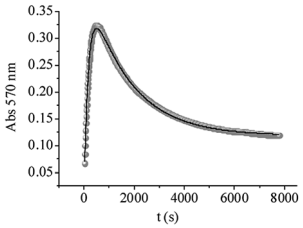

Fig. 11 Experimental curves of absorbance at 570 nm *vs.* time for QA/Cr^{VI} reactions. The experimental data were fitted using eqn (16). [QA] = 0.10 M, $[HClO_4] = 0.20$ M, $[Cr^{VI}] = 4.0 \times 10^{-3}$ M, $I = 1.0$ M, $T = 33.0$ °C, and QA/Cr^{VI} = 25/1.

According to Fig. 9B, $k_V^I = (2.22 \pm 0.3) \times 10^{-3}$ s^{-1} M^{-1} and $k_V^{II} = (7.01 \pm 0.19) \times 10^{-2}$ s^{-1} M^{-3}. For the disappearance of Cr^{VI} and Cr^V, the rate constants are specified by eqn (11) and (14), respectively.

By using CW-EPR spectroscopy, the rate constants k_6 and k_5 could be independently obtained. The EPR peak-to-peak height for Cr^V in the reaction of 0.25 M **QA** and 2.5×10^{-3} M Cr^{VI} in 0.5 M $HClO_4$ increased and decayed at 18 °C (Fig. 10). A higher modulation amplitude (2.0 G) was used to avoid superhyperfine coupling. Eqn (15) was used to fit the CW-EPR data. This equation was derived by considering consecutive first-order reactions.

$$h = Ak_6(e^{-(k_5)t} - e^{-2(k_6)t})/(2k_6 - k_5) \quad (15)$$

The parameter A depends on the spectrometer settings (modulation, gain, *etc.*).

The values of both rate constants k_5 and k_6 determined by CW-EPR were in accordance with those obtained using eqn (11) and (14), considering the experimental error and the difference in temperature. The good fitting of the data shown in Fig. 10 and that of the kinetic measurements at 350 nm (Fig. 8 and 9) indicated that the use of two different spectroscopic techniques, namely, UV/vis and CW-EPR could confirm the suggested consecutive first-order reactions shown in Scheme 1. According to the previously determined k_4 values, it can be inferred that Cr^{IV} is involved in a fast kinetic step and Cr^V persists in the **QA**/Cr^{VI} mixture.

Kinetic studies at 570 nm were also carried out for **QA**/Cr^{VI} mixtures. In these experiments, it must be considered that oxo-Cr^V–**QA** complexes are not the only absorptive species present, and Cr^{IV}, Cr^{III} and Cr^{III}–ligand species also absorb at this wavelength. Additionally, and according to our previous results, Cr^{IV} did not accumulate and did not contribute to the absorption at 570 nm. The absorbance at 570 nm *vs.* time is shown in Fig. 11. First, the absorbance increased quickly (~500 seconds) to high values, which could be associated with the formation of Cr^V and Cr^{III}–ligand complexes. After this maximum, the absorbance decayed in an exponential way. This was probably due to the decay of Cr^V species and the hydrolysis of Cr^{III}–ligand complexes. The experimental data were fitted using eqn (16), derived from Scheme 1, which considers Cr^{III}–ligand to be the final redox species in the mixture; this enabled us to confirm or reject the previous assumption.

$$Abs_{570} = \varepsilon^V[Cr^V] + \varepsilon^{III}[Cr^{III}\text{–ligand}] \quad (16)$$

Eqn (17) describes the total absorbance at 570 nm at any time.

$$Abs_{570} = \varepsilon^{III}[Cr^{VI}]_0[1 - e^{-2(k_6)t} + (\varepsilon^V - \varepsilon^{III}) k_6(e^{-(k_5)t} - e^{-2(k_6)t})/(2k_6 - k_5)] \quad (17)$$

The experimental data were properly fitted using eqn (17). The resulting calculated molar absorptivity values were $\varepsilon^V = 34$ M^{-1} cm^{-1} and $\varepsilon^{III} = 29.5$ M^{-1} cm^{-1} (Fig. 11), which were reasonable for the complexes of Cr^V and Cr^{III} with saccharides.[66] Under the experimental conditions, the values of k_6 and k_5 were in accordance with those calculated with either eqn (17) or eqn (11)–(14).

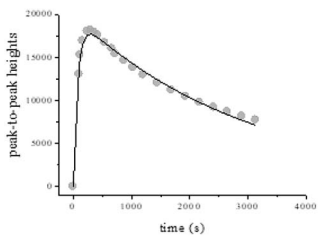

Fig. 10 EPR peak-to-peak heights for oxo-Cr^V species *vs.* time for QA/Cr^{VI} mixtures. $I = 1.0$ M, $T = 18.0$ °C, [QA] = 0.25 M, $[H^+] = 0.5$ M, $[Cr^{VI}] = 2.5 \times 10^{-3}$ M, MA = 2 G, power = 202 mW, CT = 40 ms, TC = 20 ms, and SW = 120 G.

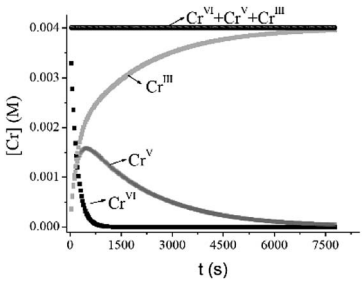

Fig. 12 Simulated kinetic profiles for Cr species. [Cr] values were calculated using $k_6 = 0.0028$ M^{-1} s^{-1}, $k_5 = 0.0005$ s^{-1}, $T = 33.0$ °C, $I = 1.0$ M, [QA] = 0.10 M, $[H^+] = 0.20$ M, and $[Cr]_T = 4.0 \times 10^{-3}$ M. Values of k_6 and k_5 were calculated using eqn (10) and (13), respectively.

The kinetic profile simulated using k_5 and k_6 shows comparable values for the time of the maximum intensity (t_{max} = 475 s) of Abs_{570} and the calculated time (465 s) at which $[Cr^V]_{max}$ occurred in the reaction (more than 40% of total Cr) (Fig. 12). These results indicate that the Cr^V intermediate species can be responsible for the behavior of the absorbance at 570 nm during the first period, whereas the next portion of the data corresponds to the slow decomposition of Cr^{III} species into $Cr^{III}_{(aq)}$. Moreover, as can be seen from Fig. 12, Cr^V still remains in the mixture after Cr^{VI} is completely consumed.

Discussion

Oxidation of QA by Cr^{VI}

The reduction of Cr^{VI} by **QA** exhibits strong pH dependence. The reaction is slow at pH > 1, and Cr^{VI} is quickly consumed when $[H^+]$ > 0.5 M. Therefore, the $[H^+]$ range of 0.1–0.05 M was preferred to perform the kinetic study of this reaction. When $[H^+]$ was 0.1 M, the time-dependent UV/vis spectra of the **QA**/Cr^{VI} mixture (Fig. 2A) showed two relevant points; the absorbance (a) decayed over time at 350 nm and 420–470 nm and (b) increased without an isosbestic point at 570 nm. As was previously pointed out, the absence of an isosbestic point indicates that more than one reaction occurs throughout the reduction of Cr^{VI} to Cr^{III}, and several chromium species are present in considerable amounts.

Kinetics analysis

The presence of Cr^{IV} and/or Cr^V intermediates during the reduction of Cr^{VI} has been previously observed for different substrates.[18,22,26,27,37] The detection of organic radicals and CrO_2^{2+} in the **QA**/Cr^{VI} mixture along with the observation of relatively long-lived oxo-Cr^V species jointly indicate that Cr^{IV}/Cr^V intermediates were produced in the reaction of **QA** with Cr^{VI}; this also strongly suggests that this redox process follows one- and two-electron pathways.

Considering the presence of the two detected chromium intermediates, namely, Cr^V and Cr^{IV} and that Cr^{IV} reacts faster than $Cr^{V/VI}$, it is necessary to determine whether both or only one of them must be considered during the analysis of experimental kinetic data. A comparison of the corresponding oxidation rates for Cr^{VI}, Cr^V and Cr^{IV} (eqn (18), (19) and (20)) can be made by employing k_n values obtained from eqn (6), (14) and (11), respectively, in the following conditions: [**QA**] = 0.03 M, $[H^+]$ = 0.1 M, and $[Cr^{IV}] = [Cr^{VI}]_T = [Cr^V]_T = 6.0 \times 10^{-4}$ M.

$$\upsilon_4 = k_4[Cr^{IV}] = (k^I_{IV} + k^{II}_{IV}[H^+]^{-1})[\mathbf{QA}][Cr^{IV}] \quad (18)$$

$$\upsilon_5 = k_5[Cr^V]_T = (k^I_V + k^{II}_V[H^+]^2)[\mathbf{QA}][Cr^V]_T \quad (19)$$

$$\upsilon_6 = k_6[Cr^{VI}]_T = (k^I_{VI} + k^{II}_{VI}[H^+]^2)[\mathbf{QA}][Cr^{VI}]_T \quad (20)$$

The calculated values of the rates were $\upsilon_4 = 1.3 \times 10^{-6}$ M s^{-1} > $\upsilon_6 = 2.3 \times 10^{-7}$ M s^{-1} > $\upsilon_5 = 5.3 \times 10^{-8}$ M s^{-1}, and the ratios between these values were (a) $\upsilon_4/\upsilon_5 \approx 25/1$, (b) $\upsilon_4/\upsilon_6 \approx 5/1$ and (c) $\upsilon_5/\upsilon_6 \approx 6/1$. These calculated data confirmed that Cr^{IV} reacted faster than Cr^V and Cr^{VI} species, suggesting that

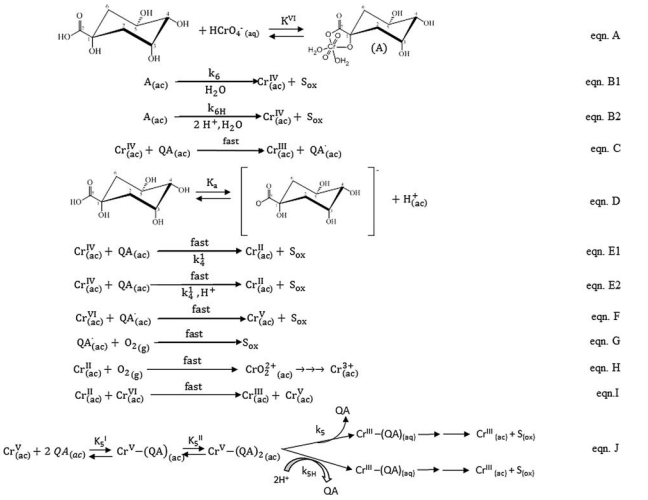

Scheme 2 Proposed mechanism of the oxidation of **QA** by Cr in acidic media.

although Cr^{IV} was formed during the oxidation of **QA** with Cr^{VI}, it did not accumulate and cannot be considered for the fitting of experimental kinetic data. The rate values calculated for υ_6 and υ_5 confirmed the kinetic profiles represented in Fig. 12, which indicated that Cr^V was still present when there was no remaining Cr^{VI}; this suggested that this intermediate species reacted more slowly than Cr^{VI} with **QA**. Consequently, at any wavelength, the time dependence of the absorption data for the reaction can be fitted using the sequence proposed in Scheme 1. Moreover, eqn (15) can be used to fit the data for CW-EPR peak-to-peak height *vs.* time (Fig. 10). The first-order rate constants determined in this way agreed perfectly with those determined from the UV/vis spectroscopy data (eqn (11) and (14)).

At this point, and considering all the previously reported results, we are able to propose and discuss a novel insight into the possible mechanism for the reaction of **QA** with Cr^{VI} (Scheme 2).

Proposed mechanism

According to the literature,[67] at $[Cr^{VI}]$ and $[H^+]$ used in these kinetic studies, Cr^{VI} occurs as $HCrO_4^-$. According to the first-order dependence on $[Cr^{VI}]$ of the reaction rate, this species is proposed to be the reactive form of Cr^{VI}. Furthermore, the oxidation reaction of alcohols with Cr^{VI} begins with the formation of Cr^{VI} esters.[26,27,37] The band observed around 460 nm shortly after **QA** and Cr^{VI} were mixed in conditions that favored the redox reaction is characteristic of the presence of the Cr^{VI} ester and indicates the presence of a Cr^{VI} complex intermediate that formed quickly prior to the reduction of Cr^{VI}. Therefore, the first step in the mechanism is the formation of the Cr^{VI} ester, where **QA** acts as a bidentate ligand (eqn A, Scheme 2). The next step in Scheme 2 is slow and comprises intramolecular two-electron transfer among molecules of the active Cr^{VI} ester to yield Cr^{IV} and S_{ox} (eqn B1 and B2). Considering that this is an acidic substrate, it can be postulated, similar to that with other substrates,[26] that both protonated and deprotonated forms of the Cr^{VI} ester can be oxidized in two

different reactions. The first reaction B1 is independent of protons, and the second reaction B2 involves two protons. The theoretical rate law for the consumption of Cr^{VI}, mathematically derived from eqn A and B in Scheme 2, is represented by eqn (21). $[Cr^{VI}]_T$ denotes the total concentration of Cr^{VI} in the mixture and takes into consideration the concentrations of the ester and aqua-chromium forms.

$$-d[Cr^{VI}]/dt = \{(k_6^{I} + k_6^{II}[H^+]^2)K^{VI}[\mathbf{QA}][Cr^{VI}]_T\}/(1 + K^{VI}[\mathbf{QA}]) \quad (21)$$

If $K^{VI}[\mathbf{QA}] \ll 1$, as can be expected considering other previously studied substrates,[26,27,37] eqn (21) becomes eqn (22), where $k_6K^{VI} = k_{VI}^{I}$ and $k_{6H}K^{VI} = k_{VI}^{II}$, which agrees with the experimental rate law (eqn (20)).

$$-d[Cr^{VI}]/dt = (k_6K^{VI} + k_{6H}K^{VI}[H^+]^2)[\mathbf{QA}][Cr^{VI}]_T \quad (22)$$

Once Cr^{IV} is formed, it participates in the oxidation mechanism in two competitive steps, comprising one- or two-electron reductions of Cr^{IV} by **QA** (eqn C and E). In eqn C, Cr^{IV} reacts in the presence of excess **QA** to generate Cr^{III} and the **QA** radical (**QA**$^{\bullet}$). This step is sustained by the polymerization of acrylamide when it is added to the **QA**/Cr^{VI} mixture. The alternative route for the reduction of Cr^{IV} by **QA** results in the formation of Cr^{II} and S_{ox}, which is supported by the detection of CrO_2^{2+} (product of the reaction of Cr^{II} with O_2). As was postulated for Cr^{VI}, **QA** exists in equilibrium between its protonated and unprotonated forms (eqn D, Scheme 2), both of which can react with Cr^{IV} in a fast reaction to yield Cr^{II} and S_{ox} (eqn E1 and E2). These are also two electron intramolecular transfers; one is independent of protons (E1) and the other involves one proton (E2). Once again, the theoretical rate law for the consumption of Cr^{IV}, which was mathematically derived from eqn D and E in Scheme 2, is described by eqn (23). $[\mathbf{QA}]_T$ represents the concentrations of the protonated and unprotonated forms of **QA**, and K_a is the acidity constant of **QA**.

$$-d[Cr^{IV}]/dt = (k_4{}^1 + k_4{}^2K_a\,[H^+]^{-1})[Cr^{IV}][\mathbf{QA}]_T \quad (23)$$

If $k_{IV}^{I} = k_4{}^1$ and $k_{IV}^{II} = k_4{}^2K_a$, this agrees with the experimental rate law (eqn (18)).

According to our results, Cr^{IV} does not accumulate in the mixture because it is involved in fast steps. The concentration of $CrO_2{}^{2+}$ should be the same as $[Cr^{VI}]_0$ if the reaction takes place entirely *via* the $Cr^{VI} \rightarrow Cr^{IV} \rightarrow Cr^{II}$ pathway.[55] Our experimental data indicate that the yield of $CrO_2{}^{2+}$ increases as the value of $[Cr^{VI}]_0$ decreases and reaches a limiting value of 49.7% (Fig. 4), indicating that nearly half of Cr^{VI} reacts *via* a route that does not involve Cr^{II}. **QA**$^{\bullet}$ and Cr^{II}, which are formed as shown in eqn C and E1 and E2, respectively, rapidly react with Cr^{VI} to produce Cr^{V} and S_{ox} in the first case (eqn F) and Cr^{V} and Cr^{III} in the second case (eqn I) ($k = 2.0 \times 10^9\ M^{-1}\ s^{-1}$).[55,68] Both species can also be quickly trapped by O_2 to give S_{ox} (eqn G) and $Cr_{(ac)}^{III}$ (eqn H). At this point, it can be seen that Cr^{V} is formed *via* two alternative routes, namely, eqn F and I, which are both fast reactions involving one-electron transfers. Once formed, Cr^{V} can further oxidize **QA** *via* a two-electron process to generate S_{ox} and Cr^{III} as the final products (eqn J, Scheme 2). As was previously demonstrated by the calculated rate values and as shown in Fig. 12, the reaction of **QA** with Cr^{V} is slower than that of **QA** with Cr^{VI} because after all the initial Cr^{VI} is consumed, Cr^{V} still remains in the mixture in measurable quantities. Based on the selectivity for the oxidation products of **QA**, the kinetic results and the CW-EPR results for the oxo-Cr^{V}–**QA** complexes,[49] we proposed a fast reaction between Cr^{V} and **QA** that produces an oxo-Cr^{V}–$(\mathbf{QA})_2$ bischelate (k_5^{I}, k_5^{II}), which finally produces S_{ox} and Cr^{III} *via* two different routes, namely, acid-dependent and acid-independent steps (eqn J). The theoretical rate law deduced for the disappearance of the Cr^{V} species (eqn (24)) is derived from eqn J in Scheme 2. $[Cr^{V}]_T$ represents the total concentration of Cr^{V} in the mixture.

$$-d[Cr^{V}]/dt = K_5^{I}K_5^{II}[\mathbf{QA}]^2(k_5^{I} + k_5^{II}[H^+]^2)\,[Cr^{V}]_T/(K_5^{I}K_5^{II}[\mathbf{QA}]^2 + K_5^{I}[\mathbf{QA}]^2) \quad (24)$$

If $K_5^{I}K_5^{II}[\mathbf{QA}]^2 \gg K_5^{I}[\mathbf{QA}]$, as can be expected considering other previously studied substrates,[26,27,37] eqn (24) becomes eqn (25), where $k_5^{I} = k_V^{I}$ and $k_5^{II} = k_V^{II}$, which agrees with the experimental rate law (eqn (19)).

$$-d[Cr^{V}]/dt = (k_5^{I} + k_5^{II}[H^+]^2)[\mathbf{QA}][Cr^{V}]_T \quad (25)$$

Conclusions

The reaction of **QA** with Cr^{VI} strongly depends on pH. The oxidation of **QA** by Cr^{VI} generates S_{ox} and a **QA**–$Cr_{(ac)}^{III}$ complex, which is then slowly hydrolyzed to form $Cr_{(ac)}^{III}$. Kinetic studies strongly support the hypothesis that the redox reaction proceeds *via* a combined mechanism, which involves $Cr^{VI} \rightarrow Cr^{IV} \rightarrow Cr^{II}$ and $Cr^{VI} \rightarrow Cr^{V} \rightarrow Cr^{III}$ pathways, as has been previously demonstrated with other substrates.[26,27,37] The mechanism is supported by the observation of $CrO_2{}^{2+}$, Cr^{V} and free radicals as reaction intermediates. The bimolecular rate constant for **QA**/Cr^{IV} reaction is much higher than that with Cr^{VI} or Cr^{V}, which proves that Cr^{IV} does not accumulate in the **QA**/Cr^{VI} reaction mixture. The detection of free radicals and the relatively long half lifetimes of Cr^{V} species are some of the reasons for warnings against the use of Cr^{VI} in industry and other human activities because of its possible role in the oxidation of several substrates that are ubiquitous in nature.

Conflicts of interest

There are no conflicts to declare.

Acknowledgements

We thank the National Research Council of Argentina (CONICET) PIP 0037, the National Agency of Scientific and Technological Promotion (ANPCyT) PICT 2016-1611, Santa Fe Province Agency of Science, Technology and Innovation ASACTEI No. AC

2015-0005, No. resol 118-16 project number 2010-174-16 and the National University of Rosario (UNR) BIO425 for financial support. We thank Roman Sapino for his help in the Cr^{IV} determination experiments and Patricia Barreto for her help in the Cr^{VI} determination experiments.

References

1 International Agency for Research on Cancer (IARC), *Overall Evaluations of Carcinogenicity to Humans, IARC, 203*, http//www.iarc.fr, OSHA, Occupational exposure to hexavalent chromium, final rule, US Department of Labor, 2006.
2 A. Levina, L. Zhang and P. A. Lay, *J. Am. Chem. Soc.*, 2010, **132**, 8720–8731.
3 B. J. Collins, M. D. Stout, K. E. Levine, G. E. Kissling, R. L. Melnick, T. R. Fennell, R. Walden, K. Abdo, J. B. Pritchard, R. A. Fernando, L. T. Bruka and M. J. Hooth, *Toxicol. Sci.*, 2010, **119**(2), 368–379.
4 J. J. Beaumont, R. M. Sedman, S. D. Reynolds, C. D. Sherman, L. H. Li, R. A. Howd, *et al.*, *Epidemiology*, 2008, **19**(1), 12–23.
5 T. Hara, T. Hoshuyama, K. Takahashi, V. Delgermaa and T. Sorahan, *Scand. J. Work, Environ. Health*, 2009, **36**(3), 216–221.
6 N. M. Gatto, M. A. Kelsh, D. Ha Mai, M. Suh and D. M. Proctor, *Cancer Epidemiol.*, 2010, **34**, 388–399.
7 D. A. Khan, S. Mushtaq, F. A. Khan and M. Q. A. Khan, *Toxicol. Ind. Health*, 2008, **29**(2), 209–215.
8 K. P. Nickensa, S. R. Patierno and S. Ceryak, *Chem.-Biol. Interact.*, 2010, **188**, 276–288.
9 L. F. Sala, J. C. Gonzalez, S. I. García, M. I. Frascaroli and S. Van Doorslaer, in *Advances in Carbohydrate Chemistry and Biochemistry*, ed D. Horton, Elsevier, Amsterdam, 1st edn, 2011, vol. 66, pp. 69–120.
10 M. Figgitt, R. Newson, I. J. Leslie, J. Fisher, E. Ingham and C. P. Casea, *Mutat. Res.*, 2010, **688**, 53–61.
11 P. A. Mazzer, L. Maurmann and R. N. Bose, *J. Inorg. Biochem.*, 2007, **101**, 44–55.
12 G. R. Borthiry, W. E. Antholine, J. M. Myers and C. R. Myers, *Chem. Biodiversity*, 2008, **5**, 1545–1557.
13 M. F. Reynolds, E. C. Peterson-Roth, I. A. Bespalov, T. Johnston, V. M. Gurel, H. L. Menard and A. Zhitkovich, *Cancer Res.*, 2009, **69**, 1–9.
14 M. D. Cohen, B. Kargacin, C. B. Klein and M. Costa, *Crit. Rev. Toxicol.*, 1993, **23**, 255–281.
15 R. Hill, A. M. Leidal, P. A. Madureira, L. D. Gillis, D. M. Waisman, A. Chiu and P. W. K. Lee, *DNA Repair*, 2008, **7**, 1484–1499.
16 T. Tanaka, S. Ohkubo, I. Tatsuno and C. Prives, *Cell*, 2007, **130**, 638–650.
17 R. Hill, A. M. Leidal, P. A. Madureira, L. D. Gillis, H. K. Cochrane, D. M. Waisman, A. Chiu and P. W. Lee, *DNA Repair*, 2008, **7**, 239–252.
18 J. C. González, M. F. Mangiameli, A. Crotta Asis, S. Bellú and L. F. Sala, *Polyhedron*, 2013, **49**, 84–92.
19 G. R Borthiry, W. E. Antholine, J. M. Myers and C. R. Myers, *J. Inorg. Biochem.*, 2008, **102**, 1449–1462.
20 A. Levina, L. Zhang and P. A. Lay, *J. Am. Chem. Soc.*, 2010, **132**, 8720–8731.
21 R. Bartholomäus, J. A. Irwin, L. Shi, S. M. Smith, A. Levina and P. A. Lay, *Inorg. Chem.*, 2013, **52**, 4282–4292.
22 L. F. Sala, J. C. Gonzalez, S. I. Garcia, M. I. Frascaroli and S. Van Doorslaer, *Adv. Carbohydr. Chem. Biochem.*, 2011, **66**, 69–120.
23 G. N. Babu, R. Ranjani, G. Farceda and S. D. S. Murthy, *J. Phytol. Res.*, 2007, **20**, 1–6.
24 A. Levina, R. Codd and P. A. Lay, in *Biological Magnetic Resonance*, ed G. R. Hanson and L. J. Berliner, Springer Publishers, New York, 2009, vol 28, Part 4, pp. 551–579.
25 J. C. González, S. I. García, S. Bellú, J. M. Salas Peregrin, A. M. Atria, L. F. Sala and S. Signorella, *Dalton Trans.*, 2010, **39**, 2204–2217.
26 M. F. Mangiameli, J. C. González, S. I. García, S. Bellú, M. Santoro, E. Caffaratti, M. I. Frascaroli, J. M. Salas Peregrín, A. M. Atria and L. F. Sala, *J. Phys. Org. Chem.*, 2010, **23**, 960–971.
27 M. F. Mangiameli, J. C. González, S. I. García, M. I. Frascaroli, S. Van Doorslaer, J. M. Salas Peregrin and L. F. Sala, *Dalton Trans.*, 2011, **40**, 7033–7045.
28 A. Levina, R. Codd and P. A. Lay, in *Biological Magnetic Resonance*, ed G. R. Hanson and L. J. Berliner, Springer Publishers, New York, 2009, vol. 28, Part 4, pp. 551–579.
29 M. Rizzotto, A. Levina, M. Santoro, S. García, M. I. Frascaroli, S. Signorella, L. F. Sala and P. A. Lay, *J. Chem. Soc., Dalton Trans.*, 2002, 3206–3213.
30 V. Roldán, J. C. González, M. Santoro, S. García, N. Casado, S. Olivera, J. C. Boggio, J. M. Salas-Peregrin, S. Signorella and L. F. Sala, *Can. J. Chem.*, 2002, **80**, 1676–1686.
31 S. Signorella, R. Lafarga, V. Daier and L. F. Sala, *Carbohydr. Res.*, 2000, **324**, 127–135.
32 S. Signorella, M. I. Frascaroli, S. García, M. Santoro, J. C. González, C. Palopoli, V. Daier, N. Casado and L. F. Sala, *J. Chem. Soc., Dalton Trans.*, 2000, 1617–1623.
33 M. Rizzotto, V. Moreno, S. Signorella, V. Daier and L. F. Sala, *Polyhedron*, 2000, **19**, 417–423.
34 M. I. Frascaroli, J. M. Salas-Peregrin, L. F. Sala and S. Signorella, *Polyhedron*, 2009, **28**, 1049–1056.
35 J. C. González, S. I. García, S. Bellú, A. M. Atria, J. M. Salas Peregrin, A. Rockenbauer, L. Korecz, S. Signorella and L. F. Sala, *Polyhedron*, 2009, **28**, 2719–2729.
36 S. E. Bellú, J. C. González, S. I. García, S. Signorella and L. F. Sala, *J. Phys. Org. Chem.*, 2008, **21**, 1059–1067.
37 M. F. Mangiameli, J. C. González, S. Bellú, F. Bertoni and L. F. Sala, *Dalton Trans.*, 2014, **43**, 9242.
38 S. Santos, C. Freire, M. Domingues, A. Silvestre and C. Pascoal, *J. Agric. Food Chem.*, 2011, **59**(17), 9386–9393.
39 J. A. Rivera, Forum Café, http://www.forumdelcafe.com/sites/default/files/biblioteca/f-45_alquimia_tueste_cafe_0.pdf.
40 R. M. Sedman, J. Beaumont, T. A. McDonald, S. Reynolds, G. Krowech and R. Howd, *J. Environ. Sci. Health, Part C: Environ. Carcinog. Ecotoxicol. Rev.*, 2006, **24**, 155–182.
41 K. Salnikow and A. Zhitkovich, *Chem. Res. Toxicol.*, 2008, **21**, 28–44.

42 A. K. Patlolla, C. Barnes, C. Yedjou, V. R. Velma and P. B. Tchounwou, *Environ. Toxicol.*, 2009, **24**(1), 66–73.
43 W. Maret and A. Wedd, *Binding Transport and Storage of Metal Ions in Biological Cells*, Science, 2014, p. 202, https://books.google.com.ar/books?isbn=1849735999.
44 S. M. Roberts, J. P. Kehrer and L. Klotz, *Studies on Experimental Toxicology and Pharmacology*, Science, 2015, ch. 9, p. 175, https://books.google.com.ar/books?isbn=3319190962.
45 A. Yokoyama, K. Cho, K. D. Karlin and W. Nam, *J. Am. Chem. Soc.*, 2013, **135**(40), 14900–14903, DOI: 10.1021/ja405891n.
46 S. K. Panda and S. Choudhury, *Braz. J. Plant Physiol.*, 2005, **17**(1), 95–102.
47 R. Codd, P. A. Lay and A. Levina, *Inorg. Chem.*, 1997, **36**, 5440–5448.
48 R. Saha, R. Nandi and B. Saha, *J. Coord. Chem.*, 2011, **64**(10), 1782–1806.
49 R. Codd and P. A. Lay, *J. Am. Chem. Soc.*, 1999, **121**, 7864–7876.
50 A. Al-Ajlouni, A. Bakac and J. H. Espenson, *Inorg. Chem.*, 1994, **33**, 1011–1014.
51 O. A. Babich and E. S. Gould, *Inorg. Chem.*, 2001, **40**, 5708–5710.
52 International Agency for Research on Cancer (IARC), *IARC Monogr. Eval. Carcinog. Risks Hum.*, Lyon, France, 1990, vol. 49, Updated 1997.
53 R. Feldam, in *Occupational and Environmental Neurotoxicology*, Lippincott-Raven Publishers, Philadelphia, 1999.
54 F. Hasan and J. Rocek, *J. Am. Chem. Soc.*, 1972, **94**, 9073–9081.
55 S. Scott, A. Bakac and J. Espenson, *J. Am. Chem. Soc.*, 1992, **114**, 4205–4213.
56 S. Scott, A. Bakac and J. Espenson, *J. Am. Chem. Soc.*, 1991, **113**, 7787–7788.
57 P. A. Lay and A. Levina, *J. Am. Chem. Soc.*, 1998, **120**, 6704–6714.
58 J. Pérez Benito, C. Arias and D. Lamrhari, *New J. Chem.*, 1994, **18**, 663–666.
59 J. Pérez Benito and C. Arias, *Can. J. Chem.*, 1993, **71**, 649–655.
60 A. B. P. Lever, in *Inorganic Electronic Spectroscopy*, Elsevier, Amsterdam, 2nd edn, 1984, p. 419.
61 M. Mitewa and P. Bontchev, *Coord. Chem. Rev.*, 1985, **61**, 241–272.
62 A. Al-Ajlouni, A. Bakac and J. H. Espenson, *Inorg. Chem.*, 1994, **33**, 1011–1014.
63 J. C. González, S. García, N. Mamana, L. F. Sala and S. Signorella, *Inorg. Chem. Commun.*, 2006, **9**, 437–440.
64 A. Nemes and A. Bakac, *Inorg. Chem.*, 2001, **40**, 2720–2724.
65 J. H. Espenson, in *Chemical Kinetcis and Reactions Mechanism*, Mc Graw Hill, New York, 2nd edn, 2002.
66 R. Codd, C. T. Dillon, A. Levina and P. A. Lay, *Coord. Chem. Rev.*, 2001, **216/217**, 537–577.
67 N. E. Brasch, D. A. Buckingham, A. B. Evans and C. R. Clark, *J. Am. Chem. Soc.*, 1996, **118**, 7969–7980.
68 O. Pestovsky, A. Bakac and J. H. Espenson, *J. Am. Chem. Soc.*, 1998, **120**, 13422–13428.